REPORT DOCUMENTATION PAGE

Form Approved
OMB No. 0704-0188

1. REPORT DATE *(DD-MM-YYYY)*	2. REPORT TYPE	3. DATES COVERED *(From - To)*
	Technical Papers	

4. TITLE AND SUBTITLE

Please see attached

5a. CONTRACT NUMBER

5b. GRANT NUMBER

5c. PROGRAM ELEMENT NUMBER

6. AUTHOR(S)

5d. PROJECT NUMBER
2303

5e. TASK NUMBER
M2C8

5f. WORK UNIT NUMBER
345709

7. PERFORMING ORGANIZATION NAME(S) AND ADDRESS(ES)

Air Force Research Laboratory (AFMC)
AFRL/PRS
5 Pollux Drive
Edwards AFB CA 93524-7048

8. PERFORMING ORGANIZATION REPORT

9. SPONSORING / MONITORING AGENCY NAME(S) AND ADDRESS(ES)

Air Force Research Laboratory (AFMC)
AFRL/PRS
5 Pollux Drive
Edwards AFB CA 93524-7048

10. SPONSOR/MONITOR'S ACRONYM(S)

11. SPONSOR/MONITOR'S NUMBER(S)
Please see attached

12. DISTRIBUTION / AVAILABILITY STATEMENT

Approved for public release; distribution unlimited.

13. SUPPLEMENTARY NOTES

14. ABSTRACT

15. SUBJECT TERMS

16. SECURITY CLASSIFICATION OF:			17. LIMITATION OF ABSTRACT	18. NUMBER OF PAGES	19a. NAME OF RESPONSIBLE PERSON
					Leilani Richardson
a. REPORT	b. ABSTRACT	c. THIS PAGE	A		19b. TELEPHONE NUMBER *(include area code)*
Unclassified	Unclassified	Unclassified			(661) 275-5015

CP

MEMORANDUM FOR PRS (In-House/Contractor Publication)

FROM: PROI (STINFO) 06 Sep 2001

SUBJECT: Authorization for Release of Technical Information, Control Number: **AFRL-PR-ED-TP-2001-182** Robert J. Hinde (Univ. of Tennessee); David T. Anderson (Univ. of Wyoming); Simon Tam; Mario E. Fajardo, "Probing Quantum Solvation W/ IR Spec.: IR Activity Induced in Solid pH_2 by N_2 and Ar Dopants"

Physical Review Letters **(Statement A)**
(Deadline: ASAP)

1. This request has been reviewed by the Foreign Disclosure Office for: a.) appropriateness of distribution statement, b.) military/national critical technology, c.) export controls or distribution restrictions, d.) appropriateness for release to a foreign nation, and e.) technical sensitivity and/or economic sensitivity.
Comments:_____

Signature _____ Date _____

2. This request has been reviewed by the Public Affairs Office for: a.) appropriateness for public release and/or b) possible higher headquarters review.
Comments: _____

Signature _____ Date _____

3. This request has been reviewed by the STINFO for: a.) changes if approved as amended, b) appropriateness of references, if applicable; and c.) format and completion of meeting clearance form if required
Comments:_____

Signature _____ Date _____

4. This request has been reviewed by PR for: a.) technical accuracy, b.) appropriateness for audience, c.) appropriateness of distribution statement, d.) technical sensitivity and economic sensitivity, e.) military/ national critical technology, and f.) data rights and patentability
Comments:_____

APPROVED/APPROVED AS AMENDED/DISAPPROVED

PHILIP A. KESSEL Date
Technical Advisor
Space and Missile Propulsion Division

Probing quantum solvation with infrared spectroscopy: infrared activity induced in solid parahydrogen by N_2 and Ar dopants

Robert J. Hinde*
Department of Chemistry, University of Tennessee, Knoxville, Tennessee 37996-1600

David T. Anderson
Department of Chemistry, University of Wyoming, Laramie, Wyoming 82071-3838

Simon Tam◊ and Mario E. Fajardo
U.S. Air Force Research Laboratory, AFRL/PRSP, Edwards Air Force Base, California 93524-7680

We present high-resolution infrared absorption spectra of solid parahydrogen matrices containing low concentrations of N_2 or Ar impurities. The spectra reveal dopant-induced absorption features that acquire infrared activity through short-range isotropic vibrational transition dipole moments arising from dopant--H_2 intermolecular interactions. These dopant-induced features provide new insights into the perturbation of the vibron bands of the H_2 matrix by chemical impurities, and thus into the physics of solvation in a quantum solid.

DOI: fauxPRL.doc PACS numbers: 33.20.Ea, 67.80.-s, 78.30.-j

Solid hydrogen and its isotopomers (HD and D_2) have long been recognized as unique cryogenic media for high-resolution spectroscopic studies of molecular rovibrational dynamics in condensed phases [1,2]. In the lowest energy state of the solid H_2 crystal, solid parahydrogen (pH_2), each H_2 molecule is in its j=0 rotational state and is therefore a spherically symmetric object with no electrostatic multipole moments. Consequently, the pH_2 crystal is bound together only by weak pH_2--pH_2 dispersion interactions, making solid pH_2 a very "soft" and nearly non-perturbing environment for molecular impurities. This has motivated recent high-resolution infrared (IR) absorption studies [2-4] of the rovibrational spectra and dynamics of dopants embedded in solid pH_2 matrices. Analysis of these spectra within the framework of crystal field theory provides valuable information on dopant--pH_2 interactions and on the microscopic nature of dopant trapping sites in the pH_2 matrix.

Complementary information can be obtained by investigating the impurity-induced changes in the IR absorption spectrum of the H_2 matrix itself. For instance, pH_2 solids containing low concentrations of j=1 orthohydrogen (oH_2) rotational "impurities" exhibit an IR absorption feature near 4153 cm^{-1} that is assigned to the pure vibrational $Q_1(0)$ transition ($v=1 \leftarrow 0$, $j=0 \leftarrow 0$) of pH_2 molecules in the matrix [5]. Although this transition is strictly IR inactive in isolated gas phase pH_2 molecules and in pure solid pH_2, orientational transitions of the oH_2 dopant's permanent quadrupole moment provide a mechanism for inducing nonzero $Q_1(0)$ transition moments in pH_2 molecules within the doped solid [6]. This oH_2-induced absorption feature has a characteristic asymmetric lineshape arising from "vibron hopping," or delocalization of the v = 1 vibrational excitation throughout the pH_2 matrix. Analysis of this lineshape provided important information on the vibrational dependence of the H_2--H_2 potential before the era of *ab initio* and molecular beam studies of intermolecular potentials [6-8].

Spherical dopants such as alkali metal and rare gas atoms can also induce IR activity in solid pH_2 matrices [9], although via a qualitatively different mechanism that originates in short-range isotropic overlap-induced transition dipole moments [10] arising from intermolecular exchange interactions. The effectiveness of this induction mechanism stems from the fact that a chemical impurity breaks the local symmetry of the pH_2 lattice; hence this mechanism is truly general, and applies to atomic and molecular impurities alike. Because the net transition moment for these induced transitions depends sensitively on the microscopic structure of the dopant trapping site [10], careful study of these spectral features can provide new insights into the nature of impurity solvation in the pH_2 quantum solid.

In this Letter, we report high-resolution investigations of the IR spectra of solid pH_2 matrices doped with N_2 impurities. Because both j=0 and j=1 N_2 rotational levels are populated in the cryogenic solid pH_2 environment, these doped matrices turn out to be good model systems for comparing the newly-identified isotropic induction mechanism with previously studied mechanisms based on transition dipoles induced by the electrostatic fields of impurity species. This is because the j=0 N_2 dopants are spherical objects with no multipolar electrostatic field, and thus act only via the short-range isotropic mechanism to induce IR activity in adjacent H_2 molecules, while the j=1 N_2 dopants (like oH_2 molecules) induce transition dipoles

in both nearby and distant pH_2 molecules by virtue of their permanent quadrupole moments. Hence two distinct induction mechanisms are active in a single sample.

We prepare millimeters-thick doped solid pH_2 samples by rapid vapor deposition [9] of flows of precooled H_2 gas and room temperature dopant gas onto a BaF_2 substrate cooled to $T \approx 2$ K by a liquid helium bath cryostat. The precooled H_2 gas emerges from a variable temperature ortho/para H_2 converter [11] typically operated at $T \approx 15$ K to produce nearly pure pH_2 gas flows with approximately 100 parts per million (ppm) of residual oH_2. In some cases we operate the converter at elevated temperatures to produce oH_2-enriched samples.

The absorption spectra of the doped pH_2 samples are recorded along the substrate normal using a Fourier transform IR spectrometer. As-deposited spectra are recorded immediately after deposition at a substrate temperature of $T \approx 2.4$ K. We then anneal the samples by raising the substrate temperature to $T \approx 4.8$ K, and record some spectra at this temperature as well. Sample thicknesses are measured to within ± 10 % (95 % confidence level) using the approach described in Ref. 12. The impurity concentrations cited here are ratios of the quantities of dopant and H_2 entering the sample chamber. These values may differ from the actual impurity concentrations in the solid (due to varying sticking efficiencies of pH_2 and dopant molecules, among other reasons) but are estimated to be within ± 40 % of the *in situ* concentrations.

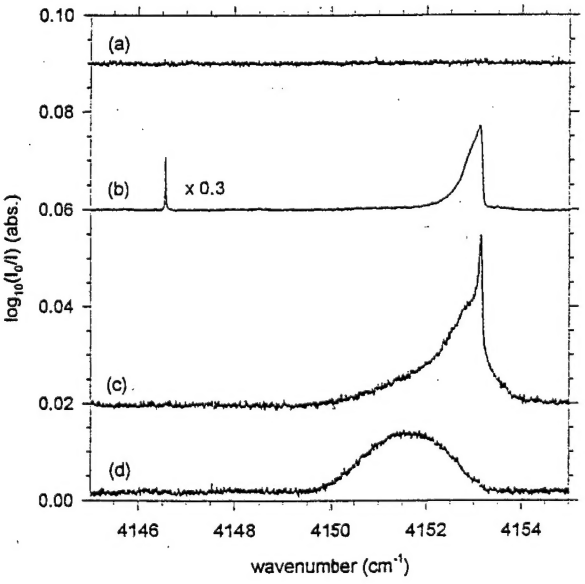

FIG. 1. Absorption spectra of four as-deposited doped pH_2 solids at $T \approx 2.4$ K. Trace (a) is for a sample containing 10 ppm of CH_4; trace (b) is for a sample containing 10 ppm of CH_4 and 2500 ppm of oH_2; trace (c) is for a sample containing 10 ppm of CH_4 and 1000 ppm of N_2; trace (d) is for a sample containing 10 ppm of CH_4 and 1000 ppm of Ar. Sample thicknesses are 2.7, 4.0, 3.1, and 2.9 mm for traces (a) through (d) respectively. Trace (b) has been scaled by a multiplicative factor of 0.3 to compensate for the higher dopant concentration and thickess of this sample. Traces (a) through (d) are presented at respective resolutions of 0.0075, 0.008, 0.01, and 0.008 cm^{-1} and have been displaced vertically for ease of presentation.

Figure 1 shows the IR absorption spectra of four as-deposited pH_2 samples. Trace (a) depicts the spectrum of a pH_2 sample containing 10 ppm of CH_4, which is included in each sample as a structural tracer for monitoring the morphology of the as-deposited samples [3,4]. No detectable IR activity in the pH_2 $Q_1(0)$ region is induced either by the CH_4 dopant (at this concentration) or by the residual oH_2 molecules present in the sample.

Trace (b) shows the absorption spectrum of solid pH_2 containing 2500 ppm of oH_2, and displays both the oH_2-induced pH_2 $Q_1(0)$ feature between 4152 and 4153.2 cm^{-1} and the narrow $Q_1(1)$ transition of the dopants themselves at 4146.6 cm^{-1}. The $Q_1(0)$ feature exhibits the asymmetric vibron hopping lineshape mentioned previously. This characteristic lineshape maps out the subset of delocalized $Q_1(0)$ vibrons whose spatial wave functions achieve nonzero overlap with the quadrupolar electrostatic field of the oH_2 dopant [6], and therefore indicates the presence of an induction mechanism based on quadrupole-induced transition moments.

Trace (c) depicts the spectrum of a pH_2 sample containing 1000 ppm of natural isotopic abundance N_2; it shows a broad, asymmetric absorption feature from about 4150 to 4154 cm^{-1}. The position of this feature coincides closely with that of the pH_2 $Q_1(0)$ transition observed in mixed oH_2/pH_2 samples, and we assign this feature to N_2-induced $Q_1(0)$ transitions of pH_2 molecules in the doped solid.

The lineshape of this feature shares some common aspects with the oH_2-induced $Q_1(0)$ feature shown in trace (b), including a relatively steep blue edge and a gently sloping red edge that meet at an absorption maximum at 4153.1 cm^{-1}. Despite these similarities, we can rule out any possibility that the feature shown in trace (c) may arise from residual oH_2 impurities, because the residual oH_2 concentration in the N_2-doped sample is too low to produce the $Q_1(1)$ feature seen at 4146.6 cm^{-1} in the oH_2-enriched sample. Furthermore, the feature shown in trace (c) is much broader at the baseline than is the oH_2-induced $Q_1(0)$ transition shown in trace (b). We therefore attribute the N_2-induced feature in trace (c) to the superposition of *two distinct* N_2-induced pH_2 $Q_1(0)$ transitions: a quadrupole-generated feature induced by $j=1$ N_2 dopants, which gives the central portion of the peak its characteristic shape, and a broader, unstructured feature induced by spherical $j=0$ N_2 dopants.

Support for this interpretation is provided by trace (d) in Fig. 1, which depicts the IR spectrum of a pH_2 sample containing 1000 ppm of Ar. The spherical Ar dopants induce a broad, structureless pH_2 $Q_1(0)$ feature visible from

4150 to 4153 cm^{-1}, much like the underlying broad feature in trace (c) that we have attributed to j=0 N_2 molecules. As we explain in more detail below, the lineshapes of spectral features attributed to the isotropic overlap induction mechanism differ from those of features arising from quadrupole induction because different subsets of the pH_2 crystal's $Q_1(0)$ vibrons are rendered IR active by the two mechanisms. This shows that careful study of these dopant-induced features can shed new light on the fundamental physics of the host pH_2 matrix.

The $Q_1(0)$ features we have attributed to the symmetry breaking isotropic induction mechanism originate in (vibrational) transition dipole moments induced by short-range intermolecular exchange interactions [10]. The same transition moments lead to collision-induced $Q_1(0)$ H_2 IR absorption in pure H_2 [13,14] and in gaseous mixtures of H_2 with other atomic and molecular species [15], and the $Q_1(0)$ pH_2 features induced by Ar and j=0 N_2 dopants thus represent solid-phase analogues of collision-induced absorption. The "collisions" which generate overlap-induced transition moments in the pH_2 matrix are simply intimate, short-range interactions between nearest-neighbor molecules in the solid. These nearest-neighbor interactions play an especially prominent role in solid pH_2 matrices because the individual pH_2 molecules in the solid undergo large-amplitude zero point motions about their nominal lattice sites [17]; this in turn amplifies the effects

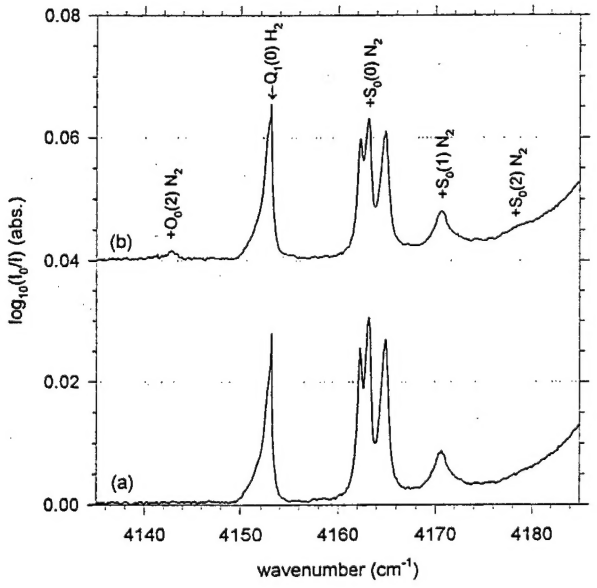

FIG. 2. Temperature dependence of the absorption spectra of the 3.1-mm-thick N_2/pH_2 sample shown in trace (c) of Fig. 1. Trace (a) is as-deposited at $T \approx 2.4$ K; trace (b) is recorded at $T \approx 4.8$ K. Both spectra are presented at 0.1 cm^{-1} resolution and have been displaced vertically for ease of presentation. The notations $+S_0(j)$ and $+O_0(j)$ represent cooperative transitions in which the pH_2 $Q_1(0)$ vibrational excitation is accompanied by a pure rotational transition of the N_2 dopant from the (v = 0, j) state to the (v = 0, j+2) and (v = 0, j-2) states, respectively.

of overlap-induced transition dipole moments, which decrease rapidly with increasing intermolecular distance [16].

Because these overlap-induced $Q_1(0)$ transition moments depend strongly on the dopant--pH_2 distance, the transitions rendered IR active by spherical dopants are those in which the final state's $Q_1(0)$ vibron has substantial amplitude on one or more of the twelve pH_2 molecules which are adjacent to the dopant. (In addition, the final state's vibron wave function must have appropriate symmetry, so that the transition moment vectors associated with these twelve pH_2 molecules do not sum to zero.) In contrast, the electrostatic field of oH_2 and j=1 N_2 dopants decays rather slowly with increasing distance (as $1/R^4$), and the quadrupole induction mechanism therefore also activates vibrons with substantial amplitudes on non-nearest-neighbor pH_2 molecules. Consequently, the spectral features induced by spherical dopants give us unique insight into the perturbation of the host crystal's vibron bands by chemical impurities, making them important tools for studying solvation in the pH_2 matrix environment.

Our interpretation of trace (c) in Fig. 1 assumes that N_2 dopants in solid pH_2 retain good rotational quantum numbers. Evidence that this is so is provided in Fig. 2, which shows the temperature dependence of four satellite IR absorption features in the vicinity of the N_2-induced $Q_1(0)$ feature. The strongest of these features is a multiplet that decreases in intensity upon heating, consisting of three peaks at 4162.3, 4163.2, and 4164.9 cm^{-1}, each 0.9 cm^{-1} wide. A weak structureless feature whose intensity is independent of temperature appears centered at 4170.6 cm^{-1} and is 1.3 cm^{-1} wide. Two very weak features, each about 4.2 cm^{-1} wide, appear when the sample is heated to $T \approx 4.8$ K: one is a doublet centered at 4142.1 cm^{-1} and the other is a shoulder centered at 4178.5 cm^{-1} superimposed on the the pH_2 Q_R phonon sideband. The spectral changes produced by heating the doped pH_2 sample are fully reversible.

As we show next, the observed temperature dependence of these satellite features, and their positions relative to the sharp maximum of the $Q_1(0)$ peak, indicate that they arise from cooperative transitions in which the pH_2 $Q_1(0)$ transition is accompanied by a pure rotational $\Delta j = 2$ transition of the N_2 dopant. This demonstrates that N_2 dopants rotate nearly freely in the pH_2 matrix.

The homonuclear N_2 molecule exists in ortho and para nuclear spin modifications associated with even and odd rotational quantum numbers, respectively [18]. In the absence of a catalyst, interconversion between orthonitrogen and paranitrogen is very slow; hence the even and odd j levels of N_2 achieve thermal equilibrium independently in the cryogenic pH_2 matrix. Although the rotational constant of N_2 dopants in the matrix environment differs slightly from that of isolated gas phase N_2 molecules (see below), this difference is small enough that we can esti-

mate the rotational level populations of N_2 dopants reasonably well using the gas phase rotational constant B_{gas} = 1.99 cm^{-1} [19]. At $T \approx 2.4$ K only the j=0 and j=1 levels of N_2 are appreciably populated, with fewer than 0.5 % of the N_2 molecules in levels with $j \geq 2$. Heating the sample to 4.8 K promotes approximately 15 % of the j=0 molecules to the j=2 level, but excites fewer than 1 % of the j=1 molecules to the j=3 level.

Consequently, the triplet feature shown in Fig. 2, which decreases in intensity by roughly 20 % upon heating, can be assigned to cooperative transitions which combine the $Q_1(0)$ pH_2 excitation with $S_0(0)$ $\Delta j = 2$ transitions of the N_2 dopant from its j=0 level. The *relative* intensities of the three peaks remain constant during the annealing cycle, confirming that the peaks arise from a common initial state that is depopulated upon heating. The triplet nature of this feature suggests that interactions between the pH_2 vibron and the N_2 dopant's j=2 rotational wave function lift the orientational degeneracy of the j=2 state. Given the approximate 1:2:2 intensity ratio of the three components of the triplet, we assign the peaks at 4162.3, 4163.2, and 4164.9 cm^{-1} to transitions to the $m_j = 0, \pm 1$, and ± 2 levels of the j=2 state, respectively.

The weak features that appear only in the spectrum of the heated sample can be assigned to cooperative transitions involving $\Delta j = \pm 2$ transitions from the N_2 j=2 level, as indicated by the $O_0(2)$ and $S_0(2)$ labels in Fig. 2. This N_2 rotational level becomes populated (at the expense of the N_2 j=0 level) when the sample is heated to $T \approx 4.8$ K. Conversely, the temperature-independent feature at 4170.6 cm^{-1} arises from cooperative transitions involving $S_0(1)$ $\Delta j = 2$ transitions from the N_2 j=1 level; the population of this N_2 level is unaffected by the thermal cycling depicted in Fig. 2.

To confirm these rotational assignments, we note that the center of gravity of the oH_2-induced $Q_1(0)$ feature [trace (b) in Fig. 1], at 4152.8 cm^{-1}, marks the vibron-free origin of the quadrupole-induced $Q_1(0)$ vibron band in solid pH_2 [6]; this represents the energy required to excite a $Q_1(0)$ transition localized on a single pH_2 molecule in the solid. The centers of gravity of the N_2-induced satellite features are shifted from this band origin by amounts corresponding to the energies of the appropriate N_2 $\Delta j = \pm 2$ rotational transitions, which are simply integer multiples of the N_2 rotational constant B in the matrix environment: 6 B for the $S_0(0)$ and $O_0(2)$ transitions, 10 B for the $S_0(1)$ transition, and 14 B for the $S_0(2)$ transition. Applying this analysis to the features shown in Fig. 2 yields $B = 1.79 \pm 0.04$ cm^{-1}, which is reduced by 10 % from B_{gas} = 1.99 cm^{-1} by crystal field effects. The good agreement among the rotational constants derived from the four satellite features indicates that the rotational assignments in Fig. 2 are internally consistent.

To summarize, we have presented high-resolution IR absorption spectra of N_2- and Ar-doped solid pH_2. The dopant-induced features observed in the spectra provide information about the solvation of small dopants in the pH_2 matrix and about the symmetry requirements and length scale of the induction mechanism generating the IR activity. In particular, the lineshapes of the dopant-induced features tell us which vibrons of the pH_2 crystal are rendered active by a particular dopant, and how the crystal's vibron bands may be perturbed by the dopant's presence.

The information encoded in these dopant-induced IR absorption spectra can be extracted with the help of quantum Monte Carlo simulations [10] which account for the highly correlated, large-amplitude zero point motions of the pH_2 solute molecules. Simulations of N_2-doped pH_2 should enable a comprehensive analysis of the lineshapes and multiplet splittings of the N_2-induced spectral features, thereby shedding light on the rotational dynamics and solvation of chemical impurities in a highly quantum solid. Further work in this direction is in progress.

This work was completed while R.J.H. and D.T.A. were visitors at the Air Force Research Laboratory's Propulsion Sciences Division (Edwards AFB), supported through contracts administered by ERC, Inc. R.J.H. acknowledges additional support from the Air Force Office of Scientific Research (contract F-49620-01-1-0068) and from the Petroleum Research Fund.

---

*Corresponding author. E-mail: rhinde@utk.edu
◊Present address: KLA-Tencor Corporation, 1 Technology Drive, Milpitas, CA 95035.

[1] T. Oka, Annu. Rev. Phys. Chem. **44**, 299 (1993).
[2] T. Momose and T. Shida, Bull. Chem. Soc. Jpn. **71**, 1 (1998).
[3] T. Momose et al., J. Chem. Phys. **107**, 7707 (1997).
[4] S. Tam et al., J. Chem. Phys. **111**, 4191 (1999).
[5] H.P. Gush et al., Can. J. Phys. **38**, 176 (1960).
[6] V.F. Sears and J. van Kranendonk, Can. J. Phys. **42**, 980 (1964).
[7] J. van Kranendonk, Can. J. Phys. **38**, 240 (1960).
[8] J. van Kranendonk and G. Karl, Rev. Mod. Phys. **40**, 531 (1968).
[9] M.E. Fajardo and S. Tam, J. Chem. Phys. **108**, 4237 (1998).
[10] R.J. Hinde, in Proceedings of the High Energy Density Matter (HEDM) Contractors Conference, Park City, Utah, October 2000 (unpublished).
[11] S. Tam and M.E. Fajardo, Rev. Sci. Instrum. **70**, 1926 (1999).
[12] S. Tam and M.E. Fajardo, Appl. Spectrosc. (submitted for publication, 2001).
[13] H.L. Welsh, M.F. Crawford, and J.L. Locke, Phys. Rev. **76**, 580 (1949).
[14] A.R.W. McKellar, J. Chem. Phys. **92**, 3261 (1990).
[15] M.F. Crawford, H.L. Welsh, J.C.F. MacDonald, and J.L. Locke, Phys. Rev. **80**, 469 (1950).
[16] G. Birnbaum, M.S. Brown, and L. Frommhold, Can. J. Phys. **59**, 1544 (1981).
[17] I.F. Silvera, Rev. Mod. Phys. **52**, 393 (1980).
[18] G. Herzberg, *Molecular Spectra and Molecular Structure. I. Diatomic Molecules*, reprint ed. (Krieger, Malabar, FL, 1989).
[19] J. Bendtsen, J. Raman Spectrosc., **2**, 133 (1974).